Nanoscale

Accepted Manuscript

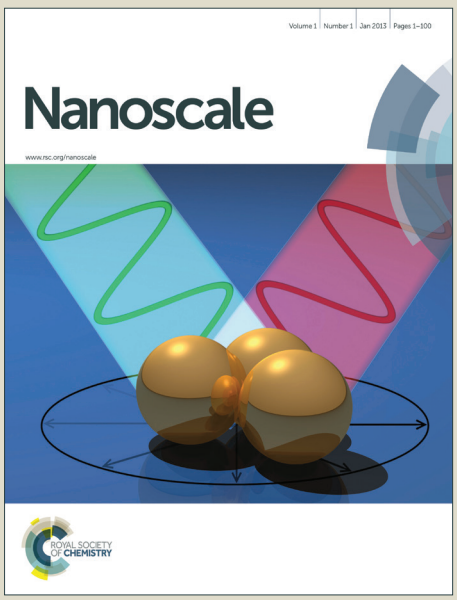

ROYAL SOCIETY OF CHEMISTRY

www.rsc.org/nanoscale

Hydroxyl PAMAM dendrimer-based gene vectors for transgene delivery to human retinal pigment epithelial cells

Panagiotis Mastorakos[§ 1,2], Siva P. Kambhampati[§ 1,2,3], Manoj K. Mishra[1,2], Tony Wu[1], Eric Song[1,4], Justin Hanes[1,2,5], Rangaramanujam M. Kannan*[1,2]

[§]**Co-first authors** with equal contribution to this work

[1]Center for Nanomedicine at the Wilmer Eye Institute, Johns Hopkins University School of Medicine, Baltimore, MD

[2]Department of Ophthalmology, Johns Hopkins University School of Medicine, Baltimore, MD

[3]Department of Biomedical engineering, Wayne State University, Detroit, MI

[4]Department of Biotechnology, Johns Hopkins University, Baltimore, MD

[5]Departments of Neurosurgery, Biomedical Engineering, Chemical & Biomolecular Engineering, Oncology, Environmental Health Sciences and Pharmacology & Molecular Sciences, Johns Hopkins University School of Medicine, Baltimore, MD

*Corresponding author:
Rangaramanujam M. Kannan, Professor of Ophthalmology, Center for Nanomedicine at the Wilmer Eye Institute, 400 North Broadway, Baltimore, Maryland 21231, USA
Tel.: +1 443-287-8634; Fax: +1 443-287-8635; e-mail: krangar1@jhmi.edu

Ocular gene therapy holds promise for the treatment of numerous blinding disorders. Despite the significant progress in the field of viral and non-viral gene delivery to the eye, important obstacles remain in the way of achieving high-level transgene expression without adverse effects. The retinal pigment epithelium (RPE) is involved in the pathogenesis of retinal diseases and is a key target for many gene-based therapeutics. In this study, we addressed the inherent drawbacks of non-viral gene vectors and combined different approaches to design an efficient and safe dendrimer-based gene delivery platform for delivery to human RPE cells. We used hydroxyl-terminated polyamidoamine (PAMAM) dendrimers functionalized with different amounts of amine groups to achieve effective plasmid compaction. We further used triamcinolone acetonide (TA) as a nuclear localization enhancer for the dendrimer-gene complex, and achieved significant improvement in cell uptake and transfection of hard-to-transfect human RPE cells. To improve serum stability, we further conjugated the dendrimer-TA with neutral polyethylene glycol (PEG). The resultant complexes showed improved stability while minimally affecting transgene delivery, thus improving the translational relevance of this platform.

Keywords: Dendrimers, Ocular Gene Delivery, Transfection, Human Retinal Pigment Epithelium, Triamcinolone acetonide.

1. Introduction

As an immune privileged and easily accessible organ, the eye constitutes a favorable target for gene therapy.[1,2] The identification of well-defined genetic targets for numerous ocular disorders such as Stargardt's disease and retinitis pigmentosa, render gene therapy a promising approach.[3-6] Indeed, gene therapy for Leber Congenital Amaurosis has demonstrated promising and long-lasting results in clinical trials.[7-8]

Many recent studies have explored viruses such as adeno-associated virus in the field of ocular gene therapy.[9-12] While relatively efficient, viral gene vectors are limited to some extent by technical difficulties in scale-up, high cost of production[13] and risk of mutagenesis.[14] Moreover, repeated administrations and prior exposures may cause neutralizing immune responses, in spite of the immune privileged environment of the eye.[15-17] The size cut-off for the expression cassette that can be packaged in viruses excludes the delivery of large transgenes that may be effective in monogenic ocular diseases.[18-20] Non-viral gene vectors constitute an alternative that can overcome most of the aforementioned limitations[21] in achieving ocular transgene delivery.[22-23] However, important issues such as vehicle cytotoxicity, instability in physiological solutions as well as low level of cellular uptake, nuclear transfer and transgene expression limit the clinical applications of nano-carriers.[24] Various cationic polymer-based gene delivery systems, such as cationic dendrimers, have demonstrated effective transgene expression *in vitro* and *in vivo*[21]. The protonable amines of these gene vectors contribute to endosome escape and allow relatively high levels of transfection.[25] However, the same amine groups that enhance transfection lead to cytotoxicity, entrapment in physiological mesh-like barriers[26-27] and tendency towards nanoparticle aggregation. For these reasons, a variety of new approaches are being explored to overcome the inherent limitations of cationic polymer based non-viral gene vectors.[21, 28]

Several dendrimers, such as polyethylenimine (PEI) and polyamidoamine (PAMAM), have been used as non-viral gene delivery vectors with relatively promising results.[29-31] Amine-terminated PAMAM dendrimers demonstrate relatively high levels of transfection but are limited by cytotoxicity due to their amine-functionalized surface.[21, 32] Hydroxyl-terminated PAMAM dendrimers demonstrate improved safety profile and have proven to be effective drug and gene delivery vehicles.[33-34] However, their near neutral surface charge and lack of protonatable amines impedes their use in nucleic acid compaction and transgene delivery.[35]

Triamcinolone acetonide (TA) is an intermediate-acting, potent corticosteroid, administered intravitreally for the treatment of sympathetic ophthalmia, temporal arteritis, uveitis and other ocular inflammatory conditions not responsive to systemic corticosteroids. Due to its neuroprotective and anti-angiogenic properties, TA has also previously been used as an adjuvant therapy for diabetic macular edema (DME), retinal vein occlusion, and some forms of age-related macular degeneration.[36-39] In direct relevance to the present studies, TA has also been suggested to improve gene vector accumulation in the nucleus, as a nuclear localization signaling agent, dilating the nuclear pores up to 60 nm when bound to its receptor.[40] Ma et al. have demonstrated that TA conjugation on PEI as well as cationic PAMAM dendrimers can significantly improve transgene expression of cationic polymer based gene vectors.[41-42]

We designed small compact gene vectors based on nearly neutral, hydroxyl-terminated PAMAM dendrimers functionalized with a minimal number of primary amine groups[43] to allow for efficient compaction while maintaining their favorable safety profile. We further utilized TA to offset the lack of protonatable amines and achieve high levels of safe transgene expression. Additionally, we used a polyethylene glycol (PEG) surface coating to enhance colloidal stability of the aforementioned gene vectors in physiological solutions. We determined the physicochemical characteristics of the dendrimer-based gene vectors and examined the effect

of the various complexation strategies on cell uptake and transfection efficiency in hard to transfect, sensitive and clinically relevant human retinal pigment epithelial cells.[44-46]

2. Materials and Methods

2.1 Materials and reagents

Hydroxyl- and amine- functionalized ethylenediamine core generation four PAMAM dendrimers (G4-OH and G4-NH_2; diagnostic grade; 64 end-groups) were purchased from Dendritech Inc. (Midland, MI, USA). TA, N-(3-dimethylaminopropyl)-N′-ethylcarbodiimide hydrochloride (EDC.HCl) glutaric anhydride, piperidine, *N,N'*-diisopropylethylamine (DIEA), trifluoroacetic acid (TFA), anhydrous dimethylformamide (DMF), dimethylacetamide (DMA), and dimethylsulfoxide (DMSO) were purchased from Sigma-Aldrich (St. Louis, MO, USA). 4-(Fmoc-amino)butyric acid (Fmoc-GABA-OH) and (benzotriazol-1-yloxy)tripyrrolidino-phosphonium hexafluorophosphate (PyBOP) were purchased from Bachem Americas Inc. (Torrance, CA, USA). Cy5-mono-NHS ester was purchased from Amersham Biosciences-GE Healthcare (Pittsburgh, PA, USA). mPEG2000 NHS ester was purchased from Creative PEGWorks (Winston Salem, NC, USA). ACS grade DMF, DMSO, dichloromethane (DCM), diethylether, hexane, ethyl acetate, HPLC grade water, acetonitrile, and methanol were obtained from Fisher Scientific and used as received. Dialysis membrane (MW cut-off 1000 Da) was obtained from Spectrum Laboratories Inc. (Rancho Dominguez, CA, USA).

2.2 Dendrimer conjugate characterization

2.2.1 Proton NMR Characterization

Proton NMR spectra of the final conjugates as well as intermediates were recorded on a Bruker (500 MHz) spectrometer using commercially available DMSO-d_6 solvents. Proton chemical shifts were reported in ppm (δ) and tetramethylsilane (TMS) used as internal standard. All data were processed using ACD/NMR processor software (Academic Edition).

2.2.2 High performance liquid Chromatography (HPLC)

The purity of the dendrimer conjugates was analyzed by HPLC (Waters Corporation, Milford, Massachusetts) equipped with a 1525 binary pump, a 2998 photodiode array (PDA) detector, a 2475 multi-wavelength fluorescence detector, and a 717 auto sampler (kept at 4°C) interfaced with Empower software. The HPLC chromatograms were monitored at 210 (G4-OH) and 240 nm (TA conjugated dendrimers) using PDA detector. Fluorescence detector was used for the detection of Cy5-conjugated dendrimer (excitation: 645 nm and emission: 662 nm). The water/acetonitrile (0.1% w/w TFA) was freshly prepared, filtered, degassed, and used as mobile phase. Symmetry C_{18} reverse-phase column, TSK gel ODS-80 Ts (250 X 4.6 mm, i.d., 5 µm) and TSK gel guard column were used for the study (Tosoh Bioscience LLC, Japan). A gradient flow was used with initial condition of 100:0 (H_2O/ACN), gradually increasing to 90:10 (H_2O/ACN) in 10 min to 50:50 (H_2O/ACN) in 20 min and returning to 100:0 (H_2O/ACN) in 50 min with flow rate of 1 mL/min for all conjugates.

2.2.3 Fluorescence spectroscopy

Fluorescence spectra of the Cy5-conjugated dendrimer (BiD-TA-Cy5) were recorded in phosphate buffer (0.1M) using a Shimadzu RF-5301 spectrofluorometer with excitation at 645 nm and emission at 662 nm. To measure the fluorescence quantum yield of BiD-TA-Cy5 the absorbance at a wavelength of 645 nm and integrated fluorescence intensity following excitation at 645 nm of Cy5-conjugated dendrimer (BiD-TA-Cy5) and free Cy5 solutions at various concentrations were measured using the Synergy Mx Monochromator-Based Multi-Mode Microplate reader (Biotek, Winooski, VT). The quantum yield was calculated using the previously described comparative method[47].

2.2.4 Measurement of size and zeta potential of the conjugates

Dendrimer conjugates were dissolved at 1mg/mL in 10 mM NaCl at pH 7.0. The ζ-potential was measured by laser Doppler anemometry using a Nanosizer ZS90 (Malvern Instruments, Southborough, MA).

2.2.5 Buffering capacity of dendrimer conjugates

Dendrimer conjugates were dissolved at a concentration of 0.2 mg/mL in 5 mL of ultrapure DI water. Ultrapure water and PEI were used as a control. The initial pH was adjusted to 12.0 using 1.0 M NaOH and the solutions were titrated at 5 µL steps of 0.1 M HCl. The pH was measured using a microprocessor-based pH meter (Hanna instruments, Woonsocket, RI).

2.3 Dendrimer conjugate synthesis

*2.3.1 Preparation of bifunctional dendrimer (BiD, **2**)*

Fmoc-functionalized dendrimer (BiD-Fmoc, ***1***) and amine functionalized bifunctional dendrimer (BiD, **2**) were synthesized as previously described.[43] A brief summary is provided as part of supplement information.

2.3.2 Synthesis of Triamcinolone acetonide-21-glutarate (TA-linker)

TA (200 mg, 0.46 mmol) was dissolved in 20 mL of DMF/DMA (8:2) in a 50 mL round bottom flask under nitrogen atmosphere. Glutaric anhydride (105 mg, 0.92 mmol) dissolved in 10 mL of DMF/DMA (80:20), and 0.2 mL of TEA were added to it and the reaction mixture was stirred for 48 h to complete the reaction. The completion of the reaction was monitored by thin layer chromatography (TLC) using ethyl acetate/methanol (80:20) as mobile phase. The solvent was evaporated under reduced pressure and the crude product was purified with column chromatography by passing through silica gel using ethyl acetate:methanol (99:1) as eluent to get TA-*21*-glutarate (220 mg, >90% yield). The obtained purified product was characterized by using ^{1}H NMR spectroscopy. ^{1}H NMR (DMSO-d_6): δ 0.84 (s, 3H, -CH_3), 1.15 (s, 3H, -CH_3), 1.35

(s, 3H, -CH_3), 1.50-1.61 (m, 5H, -CH_2 and -CH_3), 1.71-1.84 (m, 3H, -CH_2 of linker and -C*H* proton of TA), 1.94-1.97 (m, 1H, -C*H*), 2.03-2.06 (m, 1H, -C*H*), 2.30-2.36 (m, 3H, -CH_2 of linker and -C*H* protons of TA), 2.46-2.49 (t, 2H, -CH_2 protons of linker), 2.61-2.67 (m, 1H, -C*H*), 3.59 (s, 1H, -CH), 4.21 (brs, 1H, -C*H*), 4.75-4.79 (d, 1H, -C*H*), 4.86-4.87 (d, 1H, -C*H*), 5.14-5.17 (d, 1H, -C*H*), 5.49-5.50 (d, 1H, -C*H*), 6.03 (s, 1H, aromatic proton), 6.26 (d, 1H, aromatic proton), 7.29-7.31 (d, 1H, aromatic proton), 12.12 (bs, 1H, COO*H* proton).

*2.3.3 Synthesis of Fmoc-functionalized bifunctional-Triamcinolone acetonide (BiD-Fmoc-TA, **3**)*

TA-*21*-glutarate (70.6 mg, 0.129 mmol) was dissolved in 10 mL of anhydrous DMF under nitrogen atmosphere, and PyBOP (100.5 mg, 0.193 mmol) and DIEA (0.35 mL) were added to it. The reaction mixture was stirred at 0°C for 30 min. followed by the addition of BiD-Fmoc (200 mg, 0.0086 mmol) dissolved in 10 mL of DMF, and the reaction was allowed to go to completion (48 h) under nitrogen conditions. The reaction mixture was evaporated under reduced pressure and dialyzed in DMF for 24 h, while the solvent was replaced every 6 h (Dialysis membrane cutoff 1000 Da) to remove the unreacted starting materials and byproducts. The resultant DMF was evaporated, and the conjugate was dissolved in water and re-dialyzed against water for 6 h and lyophilized to get BiD-Fmoc-TA acetonide conjugate (BiD-Fmoc-TA,**3**) as an off-white color solid product (220 mg). The conjugate was characterized by 1H NMR, and the drug loading was assessed using the proton integration method. ^{1}H NMR (DMSO-d_6) δ 0.84 (s, -CH_3 protons of TA), 1.15 (s, -CH_3 protons of TA), 1.36 (s, -CH_3 protons of TA), 1.47-1.55 (m, -CH_3 and -C*H* protons of TA), 1.64 (s, -CH_2 protons of linker) 1.73-1.82 (-C*H* proton of TA), 1.92 (m, -C*H* protons of TA), 2.27 (m, -CH_2 protons of G4-OH), 2.67-3.40 (m, -C*H* protons of TA, -CH_2 protons of linker and -CH_2 protons of G4-OH), 4.00 (s, CH_2OC=O protons, G4-OH), 4.19 (brs, -C*H* protons of Fmoc group), 4.29 (bs, OCH_2 protons of Fmoc group), 4.70-6.25 (m, -OH protons

of G4-OH, -C*H* and aromatic protons of TA), 7.29-8.05 (m, carbamate protons, aromatic protons of Fmoc, aromatic protons of TA and amide protons of G4-OH).

*2.3.4 Synthesis of bifunctional-Triamcinolone acetonide (BiD-TA, **4**)*

BiD-Fmoc-TA dendrimer (220 mg) was dissolved in anhydrous DMF (10 mL) and piperidine/DMF (2:8; 10 mL) was added to it under nitrogen. The reaction mixture was stirred for 30 min. and solvent was evaporated under vacuum at room temperature. The resultant crude product was subjected to dialysis in DMF (membrane MWCO = 1 kDa) for 24 h. The solvent was evaporated and the conjugate was re-dialyzed against water for 3-4 h and lyophilized to get BiD-TA, **4**(145 mg) as off-white solid product. The BiD-TA has some free amine groups and TA molecules on the surface. ^{1}H NMR (DMSO-d_6) δ 0.83 (s, -CH_3 protons of TA), 1.15 (s, -CH_3 protons of TA), 1.35 (s, -CH_3 protons of TA), 1.50 (s, -CH_3 protons of TA), 1.54-2.07 (m, -C*H* protons of TA, -CH_2 protons of linker), 2.21 (bs, -CH_2 protons of G4-OH), 2.29-2.48 (m, -C*H* protons of TA, -CH_2 protons of linker and -CH_2 protons of G4-OH), 2.65 (bs, -CH_2 protons of G4-OH), 3.10-3.12 (t, -CH_2 protons of G4-OH), 3.28-3.29 (d, -CH_2 protons of G4-OH), 3.28-3.41 (t, -CH_2 protons of G4-OH), 4.01-4.02 (d, CH_2OC=O protons, G4-OH), 4.20-7.31 (singlet and doublet, -C*H* and aromatic protons of TA), 7.82-8.07 (m, amide protons of G4-OH).

*2.3.5 Synthesis of Cy5-labeled bifunctional-triamcinolone acetonide dendrimer (BiD-TA-Cy5, **5**)*

The BiD-TA, **4** (15.5 mg, 0.0006 mmol) was dissolved in 2 ml of borate buffer (pH 9.0) at room temperature. The reaction mixture was cooled to 0°C and Cy5 mono NHS ester (0.72 mg, 0.00091 mmol) was added dissolved in 1 ml of DMSO. The reaction mixture was stirred overnight at room temperature to complete the reaction and lyophilized. The obtained crude product was dissolved in water and subjected to dialysis against pure DI water (membrane MWCO = 1 kDa) for 8h with successive change of water in every 2h. The resultant water layer

was lyophilized to get BiD-TA-Cy5, **5**(12.8 mg). The BiD-TA-Cy5 was characterized by reverse-phase HPLC, and fluorescent spectrophotometer.

2.3.6 Synthesis of amine dendrimer-mPEG2000 conjugate (G4-NH_2-PEG, **6**)

The G4-NH_2 dendrimer (100 mg, 0.007 mmol) was dissolved in borate buffer (10 mL) and EDC●HCl (134.5 mg) was added to it at 0°C. After 10 min mPEG2000 NHS ester was added and stirred the reaction mixture for 2 h. Finally the reaction mixture was dialyzed against water for 48 h (membrane cutoff: 8 kDa) and lyophilized to get PEG-functionalized dendrimer (G4-NH_2-PEG,**6**). The final product was characterized by ^{1}H NMR, (DMSO-d_6) δ 2.15-2.65 (-CH_2 protons of G4-OH), 3.08-3.10 (-CH_2 protons of G4-OH), 3.25 (-OCH_3 protons of PEG), 3.36-3.66 (-OCH_2 protons of PEG), 8.02-8.24 (amide protons of G4-OH).

2.4 Gene vector formulation

2.4.1 Gene vector complexation

The pBAL was produced by Copernicus Therapeutics Inc. (Cleveland, OH) and pEGFP plasmid was purchased by Clontech Laboratories Inc. (Mountain View, CA). The plasmids were expanded and purified as previously described.[26] Plasmid was fluorescently labeled with Cy5 or Cy3 using Mirus Label IT® Tracker™ Intracellular Nucleic Acid Localization Kit (Mirus Bio, Madison, WI). The gene vector complexation was achieved by the drop-wise addition (1mL/min) of 10 volumes of plasmid DNA at a concentration of 0.1 mg/ml to 1 volume of a swirling polymer solution. Different polymer solutions were prepared with one or more dendrimer conjugates at nitrogen to phosphate (N/P) ratio of 5 unless otherwise specified. For the formulation of gene vectors with varying amounts of TA, blends of BiD-TA and BiD with a varying percentage of amine groups contributed by the BiD-TA polymer (100%, 75%, 50%, 25%, 10%, 5%) were used. For the formulation of PEGylated gene vectors, blends of BiD-TA and D-NH_2-PEG with a

varying percentage of amine groups contributed by D-NH_2-PEG (75%, 50%, 25%) were used. The plasmid-polymer solutions were incubated for 30 min at room temperature to allow the formation of gene vectors. PEI and PEG-poly-L-lysine (PEG-PLL) gene vectors were formulated as previously described[26] and used as controls in the following experiments.

2.4.2 Gene vector characterization

The ζ-potential of the dendrimer complexes was measured in 10 mM NaCl at pH 7.0 by laser Doppler anemometry using a Nanosizer ZS90 (Malvern Instruments, Southborough, MA). The hydrodynamic diameter and polydispersity of the gene vectors were measured in an ultrapure water solution by dynamic light scattering using a Nanosizer ZS90. In order to confirm their shape and size, the dendrimer-based gene vectors were imaged using transmission electron microscopy at 60,000x magnification (TEM, Hitachi H7600, Japan). Stability was assessed over time in ultrapure water at 4^{o}C as well as in PBS buffer in room temperature by dynamic light scattering using a Nanosizer ZS90. Gel retardation assay was preformed to assure efficient compaction of the plasmid DNA at different N/P ratios.

2.5 In vitro experiments in human retinal pigment epithelial cells

2.5.1 Cell culture

The human retinal pigment epithelial cell line (ARPE-19) was a kind gift from Dr. Gerard Lutty, Wilmer Eye Institute. Cells were cultured in Dulbecco's modified Eagle's medium, low glucose, pyruvate (DMEM, Life technologies, Grand Island, NY) supplemented with 1% penicillin/streptomycin (Invitrogen Corp., Carlsbad, CA) and 10% heat inactivated fetal bovine serum (FBS, Invitrogen Corp., Carlsbad, CA).

2.5.2 Transfection

To assess cell transfection, cells were seeded in 24-well plates at an initial concentration of 5.0×10^4 cells/well. After 24 h, cells were incubated with different dendrimer-based gene vectors carrying pBAL plasmid (2 μg of DNA/well) in media for 5 h at 37°C. Subsequently, culture media was replaced with fresh media. After additional 3 days of incubation at 37°C, media was removed and 0.5 mL of 1X Reporter Lysis Buffer was added. Cells were subjected to two freeze-and-thaw cycles to assure complete cell lysis, and supernatants were isolated by centrifugation. Luciferase activity in the supernatant was measured using a luciferase assay kit (Promega, Madison, WI) and a 20/20n luminometer (Turner Biosystems, Sunnyvale, CA). The relative light unit (RLU) was normalized to the total protein concentration of each well measured by the BCA protein assay kit (Thermo Scientific, Rockford, IL). Similarly, for image-based assessment of transfection cells were incubated with different dendrimer-based gene vectors carrying pEGFP plasmid. Two days after additional incubation at 37°C, cells were stained with NucBlue® Fixed Cell ReadyProbes® Reagent (Life Technologies, Grand Island, NY) and immediately imaged for fluorescence originated from NucBlue® and eGFP using confocal LSM 710 microscope (Carl Zeiss, Hertfordshire, UK).

2.5.3 Cell uptake/Flow cytometry

Cell uptake was assessed via flow cytometric analysis. Cells were seeded in 24-well plates at an initial concentration of 5.0×10^4 cells/well. After 24 h, cells were incubated with various dendrimer-based gene vectors carrying Cy5-labeled plasmid (2 μg DNA/well). After 5 h of incubation, the media was removed and cells were washed 3 times with 1x PBS and incubated with 1 volume of 0.25 % Trypsin with EDTA for 5 min at 37 °C. Two volumes of DMEM medium with 10% FBS were added to neutralize trypsin. The cellular uptake of gene vectors was measured using the Accuri C6 flow cytometer (BD Biosciences, San Jose, CA) with an FL4 band-pass filter with emission detection wavelength of 675/25 nm. Data were analyzed

using the BD Accuri C6 software. The thresholds were set using untreated samples; cellular uptake of dendrimer-based gene vectors was compared to that of free plasmid uptake.

2.5.4 Cell uptake/Imaging

Similarly, for image-based analysis of gene vector cellular uptake; gene vectors formulated from BiD-TA-Cy5 and Cy3-labeled plasmid were administered to cells cultured in a 35 mm glass bottom culture dish (MatTek Corporation, Ashland, MA) stained with NucBlue® Fixed Cell ReadyProbes® Reagent and imaged using confocal LSM 710 microscope over 12 h in a live cell imaging chamber.

2.5.5 Gene vector toxicity

For the assessment of gene vector toxicity, cells were seeded in 96-well plates at an initial concentration of 1.0×10^4 cells/well and incubated at 37 °C. After 24 h, cells were incubated with a range of doses of DNA gene vectors in media for 24 h at 37 °C. Cell viability was assessed using the Dojindo cell counting kit-8 (Dojindo Molecular Technologies, Inc., Rockville, MD). Absorbance at 450 nm was measured using the Synergy Mx Multi-Mode Microplate Reader (Biotek, Instruments Inc., Winooski, VT).

3. Results and Discussion

3.1 Dendrimer conjugates

*3.1.1 Preparation and characterization of the bifunctional dendrimer (BiD, **2**)*

The preparation of the bifunctional dendrimer (BiD, **2**) was prepared using Fmoc protection/deprotection chemistry as shown in Fig. 1A.[43] Our aim was to functionalize the dendrimer with approximately 20 amine groups out of the 64 hydroxyl end groups, so that it could be efficiently complexed with plasmid DNA. In brief, Fmoc-GABA-OH was reacted with the G4-OH dendrimer using PyBOP as a coupling reagent, to get Fmoc-functionalized intermediate

(BiD-Fmoc, **1**). A multiplet at 1.63 ppm for GABA-linker CH_2 protons and multiplets between 7.30-7.86 for aromatic Fmoc protons in NMR confirmed the formation of the bond. The characteristic peak at 3.99 ppm for internal CH_2 protons of G4-OH confirmed the formation of an ester bond with the linker. We calculated the loading of the linker by comparing the amidic protons of the dendrimer with aliphatic methylene protons of the linker, which suggested that 33 molecules were attached to the dendrimer. We carried out the deprotection step with piperidine (20% in DMF) without further purifying the intermediate, to get free bifunctional dendrimers (BiD, **2**). Absence of Fmoc aromatic proton peaks in NMR confirmed the deprotection of Fmoc groups. Using the proton integration method, we calculated that 18-20 linker molecules were attached to the dendrimer.

3.1.2 Preparation of Triamcinolone acetonide-21-glutarate (TA-linker)

TA was functionalized with a carboxylic acid terminal group using glutaric acid as linker since an acid group is required to conjugate with the dendrimer according to a previously published procedure.[48] In brief, TA was reacted with glutaric anhydride dissolved in DMA/DMF mixture in presence of triethylamine (TEA) as base to get the TA-linker (Fig. 1B). The TA-linker was characterized by ^{1}H NMR. TA has two reactive hydroxyl groups and the most reactive 21-position hydroxyl group has reacted with glutaric acid via ester bond. Apart from the protons signal from TA, an additional multiplet at 1.79 (CH_2 protons of linker), and two triplets at 2.32 and 2.47 (CH_2 protons of linker) confirmed the formation of the TA-linker. A characteristic peak at 12.12 ppm belonging to carboxylic acid confirmed that TA-linker has one acid group (Fig. S1).

*3.1.3 Preparation of bifunctional-TA conjugate (BiD-TA, **4**)*

Synthesis of BiD-TA was performed using a three-step process with glutaric acid as a spacer, starting from G4-OH (Fig. 1A). The Fmoc-functionalized dendrimer was reacted with TA-linker using PyBOP as the coupling reagent and DIEA as the base to get BiD-Fmoc-TA (**3**).

The conjugate was characterized by ^{1}H NMR and reverse phase HPLC. In the ^{1}H NMR spectrum, peaks at 0.84-1.50 ppm represent methyl protons of TA, and peaks at 4.75-6.25 ppm represent aromatic protons of TA and along with dendrimer peaks confirmed the formation of the conjugate. Four multiplets belonging to Fmoc aromatic protons still remained in the spectrum between 7.29 to 7.86 ppm, confirming the presence of Fmoc-linker molecules. The payload of TA to the surface of the dendrimer was calculated by comparing the proton integration of the amide protons of the G4-OH to the aromatic proton of TA; approximately 10 molecules of TA were conjugated (Fig. S2). Finally, the Fmoc groups were deprotected with piperidine (20% in DMF) to get bifunctional-TA dendrimer (BiD-TA, **4**) and the structure was established in proton NMR. Absence of aromatic Fmoc protons signal in NMR and presence of all signals related to TA confirmed the formation of the product with free amines on the surface. In the final BiD-TA conjugate, 8 molecules of TA and 23 free amine groups were confirmed using the proton integration method (Fig. S3). The lower number of TA and amine groups in the conjugate were due to hydrolysis of the ester bond with prolonged exposure to dialysis in DMF under basic conditions (presence of piperidine in the reaction mixture and traces of water in DMF). The BiD-TA conjugate was readily soluble in PBS buffer and saline solution, in contrast to TA which has poor water solubility. The retention time of BiD-TA in HPLC chromatogram at 20.1 min (monitored at 240 nm, PDA detector) confirms the conjugation of the TA to the dendrimer. At the same time, the retention time of BiD was 9.5 min (monitored at 210 nm).

*3.1.4 Preparation of BiD-TA-Cy5 (**5**) conjugate*

The BiD-TA (**4**) was labeled with Cy5, a near IR imaging agent, to study the internalization of the conjugate in RPE cells. We have previously reported the preparation of the dendrimer-Cy5 and characterized extensively using HPLC/GPC, NMR and fluorescence spectroscopy.[49] In brief, Cy5-mono-NHS ester was reacted with TA-functionalized bifunctional dendrimer (BiD-TA) in borate buffer to get Cy5-labeled dendrimers BiD-TA-Cy5 as shown in Fig.

1A. The final conjugate was purified by dialysis followed by GPC fractionation and characterized by reverse-phase HPLC and fluorescence spectroscopy. The HPLC trace showed a peak at 20.4 min. for BiD-TA-Cy5 (monitored at 645 nm excitation) different from BiD-TA and Cy5, confirming the formation of the conjugate. The fluorescence spectrum showed peaks at 648 nm (for excitation) and 663 nm (for emission) which follow a similar pattern to Cy5 also suggesting the conjugation of Cy5 to the dendrimer. Only one mole equivalent of Cy5 was used in each reaction and the percentage payload of the Cy5 to the dendrimer is ~4-5 wt%. The fluorescence quantum yield for the final conjugate was calculated to be 0.18, demonstrating a slight decrease compared to free Cy5 (~0.28).

*3.1.5 Preparation of D-NH_2-PEG (**6**) conjugate*

The amine functionalized dendrimer (D-NH_2) was partially functionalized with 2K PEG to enhance the transfection efficiency of the dendrimer. In brief, NHS-ester of mPEG2000 was reacted with D-NH_2 dissolved in borate buffer to get the PEG functionalized dendrimer and was characterized by proton NMR. In the NMR chart, a peak at 3.25 ppm corresponds to OCH_3 peak of the PEG and multiplets between 3.36-3.66 ppm (methylene protons of PEG) along with dendrimer protons peaks in between 2.15-3.10 ppm confirm the formation of the conjugate. The loading of the PEG to the dendrimer was calculated by comparing the amidic protons of the dendrimer (8.02-8.24) to the backbone methylene protons of the PEG and found out that 7 molecules of the PEG were conjugated to the dendrimer.

3.1.6 Surface charge of dendrimer conjugates

BiD-TA and BiD ζ-potential were measured to be 13.9 mV and 12.9 mV, respectively. Their surface charge was significantly lower than the ζ-potential of D-NH_2 (22.2 mV). D-NH_2-PEG demonstrated significant shielding of the D-NH_2 positive surface charge resulting in a ζ-potential of 11.7 mV.

3.1.7 *Dendrimer conjugates buffering capacity*

As expected, BiD-TA and BiD demonstrated significantly lower buffering capacity in comparison to D-NH_2 and PEI, suggesting limited ability to buffer the lysosome environment and achieve endosome escape through the proton buffer effect, hence, underlying the importance of the incorporation of TA in order to improve the nuclear localization and transfection efficiency (Fig. S4).

3.2 Gene vector formulation and characterization

Using BiD as a base, we were able to formulate compact ~50 nm gene vectors with a nearly homogeneous size distribution (PDI: 0.16). Similarly, the conjugation of 8 TA molecules did not appear to affect the complexation efficiency of these gene vectors, resulting in BiD-TA particles of similar size (~44 nm). We compared these gene vectors with conventional amine-terminated PAMAM dendrimer-based gene vectors at the same N/P ratio. This formulation resulted in particles with similar physicochemical characteristics (Fig. 2A &B and Table 1). We confirmed the spherical morphology and efficient plasmid compaction of these gene vectors using TEM (Fig. 2C). The gene vectors were stable in an aqueous solution for at least 10 days (Fig. 2E). However, once added into a high ionic strength solution (phosphate buffered saline, PBS), the particles rapidly aggregated and lost their colloidal stability. After one hour of incubation in PBS, BiD and BiD-TA reached a size of ~500 nm. D-NH_2 gene vectors aggregated at a slower rate and were ~300 nm in size at 1 hour (Fig. 2F). To achieve successful transgene expression the gene vectors need to reach the target cells intact; the lack of stability and rapid aggregation imposes a serious obstacle to *in vivo* gene therapy.

In order to improve nanoparticle stability we formulated gene vectors using a blend of BiD-TA and D-NH_2-PEG.[26] This technique resulted in gene vectors of similar size (~50 nm) but a significantly lower ζ-potential of ~6 mV in comparison to that of non-coated nanoparticles

(BiD-TA: ~11.4mV, BiD: ~13.3 mV, D-NH_2: ~14.5 mV). The ratio of BiD-TA to D-NH_2-PEG did not affect the physicochemical characteristics of the gene vectors (Fig. 2A &B and Table 1). Gene vectors formulated by 100% D-NH_2-PEG had size of 42 nm and ζ-potential of 5.2 mV. In comparison, BiD-TA/ D-NH_2-PEG based gene vectors formulated with 25%, 50% and 75% of amines contributed by BiD-TA had sizes of 51 nm, 51 nm and 43 nm, respectively and ζ-potential of 7.3 mV, 6.1 mV and 5.9 mv, respectively. The 'shielding' of the gene vectors ζ-potential suggests effective PEG coating. PEG significantly improved stability in high ionic strength solutions, as PEG coated gene vectors retained their physicochemical properties for at least 18 h. Interestingly, gene vectors with higher than 25% of amines contributed by D-NH_2-PEG slightly increased in size, whereas gene vectors with only 25% of amines contributed by D-NH_2-PEG retained their size over 18 h (Fig. 2F).

3.3 Gene vector cell uptake and transfection efficiency in retinal pigment epithelium

Transfection of BiD and BiD-TA was compared to D-NH_2 gene vectors as well as PEI and PEG-PLL gene vectors, which are widely used and are considered to be gold standards for non-viral gene delivery.[21, 50-51] The use of BiD resulted in approximately 59-, 59000- and 29000-fold lower transfection efficiency in comparison to PEG-PLL, PEI and D-NH_2 respectively, in primary RPE cells. In contrast, incubation of BiD-TA gene vectors resulted in ~1700- fold higher transfection in comparison to PEG-PLL, and no statistically significant difference in transgene expression in comparison to PEI or D-NH_2. BiD-TA transfection efficiency was 100000-fold higher than BiD (Fig. 3A), underlying the important role of TA in improving transfection efficiency. These results were qualitatively confirmed using eGFP plasmid in combination with fluorescence microscopy (Fig. 3B-D), which suggested that BiD-TA and D-NH_2 were comparable.

TA binds to the cytosolic glucocorticoid receptor (GR), which dilates the nuclear pores and translocate itself into the nucleus along with the gene carrier. [41-42] Here, we take advantage

of the high concentration of GR in human ARPE cells to achieve high-level transgene expression using hydroxyl terminated PAMAM dendrimer-based gene vectors.

Flow cytometry analysis was performed to assess the effect of different dendrimer types as well as the addition of TA on the gene vector cell uptake. BiD did not efficiently penetrate ARPE cells, with only ~30% of cell population taking up the fluorescently labeled plasmid, ~2.4-fold lower than D-NH_2. The mean fluorescence intensity (MFI) of the BiD treated cells was 100-fold lower than D-NH_2 treated cells. In contrast, BiD-TA based gene vectors achieved high level cell uptake of ~80%, comparable to D-NH_2. However, the MFI, indicative of the absolute amount of plasmid taken up, was 5-fold lower than D-NH_2 treated cells (Fig. 4A-E). This is the first study to demonstrate not only improved transfection but also enhanced cellular uptake of TA conjugated gene vectors.

In order to confirm that the nanoparticles were able to enter the cells intact, we formulated BiD-TA gene vectors with 5% of amines contributed by Bi-D-Cy5 and Cy3-labeled plasmid. Fluorescence confocal microscopy and differential interference contrast (DIC) microscopy were combined to observe co-localized Cy3-plasmid and Cy5-dendrimer in the cell cytoplasm as well as the cell nucleus, indicating that dendrimer nanoparticles were able to be taken up and localize in the nucleus intact (Fig. 4F), without disintegration during the endocytotic, and endosomal-lysosomal-nucleus transport.

3.4 Role of TA and PEG in cell uptake and transfection efficiency

In order to further understand the amount of TA required for effective cell uptake and transgene delivery, we repeated the cell uptake and transfection studies using dendrimer nanoparticles formulated from a blend of BiD-TA and BiD at a decreasing percent of amines contributed by BiD-TA (Fig. 5A-H). Varying the BiD-TA to BiD ratio did not result in significant change of the gene vector physicochemical characteristics (Table S1). More specifically, formulation of nanoparticles with 100%, 75%, 50%, 25%, 10% and 5% of amines contributed by

D-TA resulted in sizes of 42.9 nm, 34 nm, 34.5 nm, 38.8 nm, 46.2 nm and 45.8 nm, respectively. Also, the ζ-potentials were 16.5 mV, 9.92 mV, 15.8 mV, 13.6 mV, 15.3 mV, 16.9 mV, respectively. Both the percentage of cell uptake as well as MFI demonstrated a positive correlation with the percentage of BiD-TA in the gene vectors (R^2: 0.842, $p<0.01$; R^2: 0.923, $p<0.01$; respectively). The transgene expression demonstrated a similar positive correlation (R^2: 0.765, $p<0.01$). Importantly, the inclusion of BiD-TA equal to or lower than 10% did not seem to improve transfection over BiD gene vectors. This underlines the importance of achieving a significant TA concentration on the gene vector surface in order to allow for improvement of cell uptake and transgene expression.

Having established the role of a PEG coating in drastically improving the stability of these gene vectors we attempted to determine the effect of formulating a gene vector with a blend of D-NH_2-PEG and BID-TA on cell uptake and transfection efficiency. We used a previously established blending technique, with different percentages of amines contributed by D-NH_2-PEG, and achieved effective PEG coating of the gene vectors as demonstrated by the significant shielding of the positive surface charge (Table 1) and stability of the gene carriers. Flow cytometric analysis determined no significant difference in percentage of cell uptake or MFI between PEG coated gene vectors with varying ratios of D-NH_2-PEG to BiD-TA (Figure 6A-E). The percentage of cell uptake of the PEGylated dendrimer gene vector did not differ significantly from BiD-TA and D-NH_2 gene vector uptake (~80%). However, the MFI was significantly lower for the PEGylated gene vectors ($p<0.05$), indicating lower absolute amount of gene vector uptake. No difference in transfection efficacy was observed between the PEGylated gene vectors. The transgene expression following incubation with PEGylated gene vectors was significantly decreased compared to BiD-TA and D-NH_2 ($p<0.05$) but still significantly higher than BiD-based gene vectors ($p<0.05$) (Figure 6F). These findings are in good agreement with previous studies demonstrating that relatively small nanoparticles can be efficiently taken up

regardless of their PEGylation profile. However, the improved stability of PEG coated cationic polymer based gene vectors impedes endosome escape and reduces transfection.[52]

3.5 Cytotoxicity profile

ARPE cell transfection has been greatly limited by the cytotoxic effect of different gene vector systems. Importantly, cell incubation with varying concentrations of BiD-TA, BiD and BiD-TA/D-NH_2-PEG blend did not result in significant toxicity. However, incubation with D-NH_2, D-NH_2-PEG and BiD-TA/D-NH_2 blend resulted in statistically significant toxicity, presumably due to the increased positive surface charge and cytotoxicity of the base polymers (Fig. S5). Therefore, partial PEGylation and the hydroxyl groups improves the toxicity profile of the delivery vectors.

4. Conclusion

In this study we attempted to address the inherent limitations of cationic-polymer based non-viral gene vectors. Using hydroxyl-functionalized PAMAM dendrimers, we achieved effective plasmid compaction, resulting in relatively small complexes using (a) a base-polymer with minimal amount of primary amine groups to minimize cytotoxicity, (b) TA as a nuclear localization signal to improve transfection and (c) a hydrophilic and near neutral PEG coating to improve stability in physiological solutions. We demonstrated efficient transgene delivery in hard to transfect human retinal pigment epithelial cells.

Cationic polymers with a high number of amine groups, such as PEI and amine-terminated PAMAM dendrimers, have traditionally been used for efficient complexation.[21] We establish a new approach in which we minimally functionalized a hydroxyl PAMAM dendrimer, with or without the conjugation of TA, in order to achieve efficient compaction while retaining a reduced cytotoxicity profile in primary RPE cells.[53] These complexes demonstrate physicochemical characteristics similar to conventional D-NH_2 gene vectors. However, the lack

of stability of both conventional and BiD based gene vectors in high ionic strength solutions somewhat limits their translational relevance. For this reason, we adapted a previously established blending technique[26] to introduce a hydrophilic PEG coating which substantially reduces aggregation of the particles and increases the possibility of reaching the target cells intact,[26-27] allowing for protection of the plasmid cargo[54] and more efficient cell uptake.

TA has previously demonstrated the ability to improve transgene expression and nuclear localization in human embryonic kidney and human hepatocellular carcinoma.[41-42] In this study we used this attribute in order to offset the lack of buffering capacity, endosome escape and nuclear localization of BiD-based gene vectors and improve transgene expression in primary RPE cells, an important group of cells in retinal function and retinal diseases. Indeed, BiD-TA based gene vectors were observed to enter the nucleus intact and achieved high level transgene expression similar to conventional D-NH_2 based gene vectors. We demonstrate for the first time that TA can drastically enhance transfection of hard to transfect retinal pigment epithelial cells. We further show that the effect of TA is dose dependent and that at least 25% of base-polymer needs to be conjugated to TA to significantly improve transgene delivery.

The ability of gene vectors to enter the cells constitutes an important limiting factor for non-viral gene delivery for slowly replicating cells. We found that BiD based gene vectors are taken up significantly less than D-NH_2 gene vectors, presumably due to reduced electrostatic interaction with the cell membrane. Interestingly, TA seems to be involved in the endocytosis process as there was a significant improvement in cell uptake for BiD-TA based gene vectors. In fact, there was a positive correlation between the amount of TA on nanoparticles and cell uptake. This phenomenon may be attributed to the nuclear localization of BiD-TA gene vectors leading to decreased exocytosis.[55]

PEG coating has been suggested to reduce particle uptake by cells.[56-57] However, in good agreement with previous studies on PEGylated cationic polymer based gene vectors,[52] we found that PEGylation did not affect cellular uptake. Their small particle size may contribute to

effective uptake in spite of PEGylation.[58-59] The reduced transfection efficacy of the PEGylated gene vectors may be explained by their improved stability that impedes DNA unpackaging and endosome escape.[52, 60] The stability in physiological solutions, favorable safety profile and relatively high transfection efficiency of these PEGylated gene vectors renders them a promising vehicle for the delivery of therapeutic transgenes to retinal pigment epithelial cells *in vivo*.

Acknowledgements

The authors would like acknowledge Fan Zhang for insightful discussion regarding HPLC characterization of the dendrimer conjugates and Miguel Sobral for his advice in manuscript editing. Funding from NIH NIBIB (1R01EB018306-01, RMK), and Research to Prevent Blindness (RPB) is gratefully acknowledged.

References

1. M. M. Liu, J. Tuo, and C. C. Chan, *The British journal of ophthalmology.* 2011, **95,** 604.
2. S. P. Kambhampati, and R. M. Kannan, *Journal of ocular pharmacology and therapeutics : the official journal of the Association for Ocular Pharmacology and Therapeutics.* 2013, **29**.
3. V. Berry, P. Francis, S. Kaushal, A. Moore, and S. Bhattacharya, *Nature genetics.* 2000, **25,** 15.
4. G. J. Farrar, P. F. Kenna, and P. Humphries, *The EMBO journal.* 2002, **21,** 857.
5. P. A. Ferreira, *Human molecular genetics.* 2005, **14,** 259.
6. R. S. Molday, *Investigative ophthalmology & visual science.* 1998, **39,** 2491.
7. S. G. Jacobson, A. V. Cideciyan, R. Ratnakaram, E. Heon, S. B. Schwartz, A. J. Roman, M. C. Peden, T. S. Aleman, S. L. Boye, A. Sumaroka, T. J. Conlon, R. Calcedo, J. J. Pang, K. E. Erger, M. B. Olivares, C. L. Mullins, M. Swider, S. Kaushal, W. J. Feuer, A. Iannaccone, G. A. Fishman, E. M. Stone, B. J. Byrne, and W. W. Hauswirth, *Archives of ophthalmology.* 2012, **130,** 9.
8. F. Testa, A. M. Maguire, S. Rossi, E. A. Pierce, P. Melillo, K. Marshall, S. Banfi, E. M. Surace, J. Sun, C. Acerra, J. F. Wright, J. Wellman, K. A. High, A. Auricchio, J. Bennett, and F. Simonelli, *Ophthalmology.* 2013, **120,** 1283.
9. D. C. Chung, V. Lee, and A. M. Maguire, *Current opinion in ophthalmology.* 2009, **20,** 377.
10. F. Rolling, *Gene therapy.* 2004, **11,** 26.
11. Y. Chen, G. Moiseyev, Y. Takahashi, and J. X. Ma, *Investigative ophthalmology & visual science.* 2006, **47,** 1177.
12. G. D. Aguirre, V. Baldwin, S. Pearce-Kelling, K. Narfstrom, K. Ray, and G. M. Acland, *Molecular vision.* 1998, **4,** 23.
13. C. E. Thomas, A. Ehrhardt, and M. A. Kay, *Nature reviews. Genetics.* 2003, **4,** 346.
14. N. J. Olsen, and C. M. Stein, *The New England journal of medicine.* 2004, **350,** 2167.
15. X. Xiao, J. Li, and R. J. Samulski, *Journal of virology.* 1996, **70,** 8098.
16. T. B. Lentz, S. J. Gray, and R. J. Samulski, *Neurobiology of disease.* 2012, **48,** 179.

17. N. Chirmule, W. Xiao, A. Truneh, M. A. Schnell, J. V. Hughes, P. Zoltick, and J. M. Wilson, *Journal of virology.* 2000, **74,** 2420.
18. Z. J. Wu, H. Y. Yang, and P. Colosi, *Molecular Therapy.* 2010, **18,** 80.
19. H. Bitner, L. Mizrahi-Meissonnier, G. Griefner, I. Erdinest, D. Sharon, and E. Banin, *Investigative ophthalmology & visual science.* 2011, **52,** 5332.
20. C. E. Briggs, D. Rucinski, P. J. Rosenfeld, T. Hirose, E. L. Berson, and T. P. Dryja, *Investigative ophthalmology & visual science.* 2001, **42,** 2229.
21. M. A. Mintzer, and E. E. Simanek, *Chemical reviews.* 2009, **109,** 259.
22. J. C. Sunshine, S. B. Sunshine, I. Bhutto, J. T. Handa, and J. J. Green, *Plos One.* 2012, **7,** 37543.
23. R. Farjo, J. Skaggs, A. B. Quiambao, M. J. Cooper, and M. I. Naash, *Plos One.* 2006, **1,** 38.
24. M. de la Fuente, B. Seijo, and M. J. Alonso, *Gene therapy.* 2008, **15,** 668.
25. A. Akinc, M. Thomas, A. M. Klibanov, and R. Langer, *The journal of gene medicine.* 2005, **7,** 657.
26. J. S. Suk, A. J. Kim, K. Trehan, C. S. Schneider, L. Cebotaru, O. M. Woodward, N. J. Boylan, M. P. Boyle, S. K. Lai, W. B. Guggino, and J. Hanes, *Journal of controlled release : official journal of the Controlled Release Society.* 2014, **178,** 8.
27. Q. Xu, N. J. Boylan, J. S. Suk, Y. Y. Wang, E. A. Nance, J. C. Yang, P. J. McDonnell, R. A. Cone, E. J. Duh, and J. Hanes, *Journal of controlled release : official journal of the Controlled Release Society.* 2013, **167,** 76.
28. A. Pathak, S. Patnaik, and K. C. Gupta, *Biotechnology journal.* 2009, **4,** 1559.
29. W. Ke, K. Shao, R. Huang, L. Han, Y. Liu, J. Li, Y. Kuang, L. Ye, J. Lou, and C. Jiang, *Biomaterials.* 2009, **30,** 6976.
30. V. Reebye, P. Saetrom, P. J. Mintz, K. W. Huang, P. Swiderski, L. Peng, C. Liu, X. Liu, S. Lindkaer-Jensen, D. Zacharoulis, N. Kostomitsopoulos, N. Kasahara, J. P. Nicholls, L. R. Jiao, M. Pai, D. R. Spalding, M. Mizandari, T. Chikovani, M. M. Emara, A. Haoudi, D. A. Tomalia, J. J. Rossi, and N. A. Habib, *Hepatology.* 2014, **59,** 216.
31. M. L. Patil, M. Zhang, and T. Minko, *ACS nano.* 2011, **5**.
32. V. Shah, O. Taratula, O. B. Garbuzenko, M. L. Patil, R. Savla, M. Zhang, and T. Minko, *Current drug discovery technologies.* 2013, **10**.
33. S. Kannan, H. Dai, R. S. Navath, B. Balakrishnan, A. Jyoti, J. Janisse, R. Romero, and R. M. Kannan, *Science translational medicine.* 2012, **4,** 130.
34. M. L. Patil, M. Zhang, O. Taratula, O. B. Garbuzenko, H. He, and T. Minko, *Biomacromolecules.* 2009, **10**.
35. J. H. Lee, Y. B. Lim, J. S. Choi, Y. Lee, T. I. Kim, H. J. Kim, J. K. Yoon, K. Kim, and J. S. Park, *Bioconjugate chemistry.* 2003, **14,** 1214.
36. E. M. Becerra, F. Morescalchi, F. Gandolfo, P. Danzi, G. Nascimbeni, B. Arcidiacono, and F. Semeraro, *Current drug targets.* 2011, **12,** 149.
37. M. J. Elman, L. P. Aiello, R. W. Beck, N. M. Bressler, S. B. Bressler, A. R. Edwards, F. L. Ferris, 3rd, S. M. Friedman, A. R. Glassman, K. M. Miller, I. U. Scott, C. R. Stockdale, and J. K. Sun, *Ophthalmology.* 2010, **117,** 1064.
38. J. B. Jonas, *Ophthalmic research.* 2006, **38,** 218.
39. R. W. Beck, A. R. Edwards, L. P. Aiello, N. M. Bressler, F. Ferris, A. R. Glassman, E. Hartnett, M. S. Ip, J. E. Kim, and C. Kollman, *Archives of ophthalmology.* 2009, **127,** 245.
40. V. Shahin, L. Albermann, H. Schillers, L. Kastrup, C. Schafer, Y. Ludwig, C. Stock, and H. Oberleithner, *Journal of cellular physiology.* 2005, **202,** 591.
41. K. Ma, M. Hu, M. Xie, H. Shen, L. Qiu, W. Fan, H. Sun, S. Chen, and Y. Jin, *The journal of gene medicine.* 2010, **12,** 669.
42. K. Ma, M. X. Hu, Y. Qi, J. H. Zou, L. Y. Qiu, Y. Jin, X. Y. Ying, and H. Y. Sun, *Biomaterials.* 2009, **30,** 6109.

43. M. K. Mishra, C. A. Beaty, W. G. Lesniak, S. P. Kambhampati, F. Zhang, M. A. Wilson, M. E. Blue, J. C. Troncoso, S. Kannan, M. V. Johnston, W. A. Baumgartner, and R. M. Kannan, *ACS nano.* 2014, **8,** 2134.
44. A. del Pozo-Rodriguez, D. Delgado, M. A. Solinis, A. R. Gascon, and J. L. Pedraz, *International journal of pharmaceutics.* 2008, **360,** 177.
45. K. Abul-Hassan, R. Walmsley, and M. Boulton, *Current eye research.* 2000, **20,** 361.
46. A. Urtti, J. Polansky, G. M. Lui, and F. C. Szoka, *Journal of drug targeting.* 2000, **7,** 413.
47. J. R. Lakowicz, *Sub-cellular biochemistry.* 1988, **13**.
48. R. Iezzi, B. R. Guru, I. V. Glybina, M. K. Mishra, A. Kennedy, and R. M. Kannan, *Biomaterials.* 2012, **33,** 979.
49. W. G. Lesniak, M. K. Mishra, A. Jyoti, B. Balakrishnan, F. Zhang, E. Nance, R. Romero, S. Kannan, and R. M. Kannan, *Molecular pharmaceutics.* 2013, **10**.
50. D. M. Yurek, A. M. Fletcher, G. M. Smith, K. B. Seroogy, A. G. Ziady, J. Molter, T. H. Kowalczyk, L. Padegimas, and M. J. Cooper, *Molecular therapy : the journal of the American Society of Gene Therapy.* 2009, **17,** 641.
51. M. W. Konstan, P. B. Davis, J. S. Wagener, K. A. Hilliard, R. C. Stern, L. J. Milgram, T. H. Kowalczyk, S. L. Hyatt, T. L. Fink, C. R. Gedeon, S. M. Oette, J. M. Payne, O. Muhammad, A. G. Ziady, R. C. Moen, and M. J. Cooper, *Human gene therapy.* 2004, **15,** 1255.
52. S. Mishra, P. Webster, and M. E. Davis, *European journal of cell biology.* 2004, **83,** 97.
53. G. Thiagarajan, K. Greish, and H. Ghandehari, *European journal of pharmaceutics and biopharmaceutics : official journal of Arbeitsgemeinschaft fur Pharmazeutische Verfahrenstechnik e.V.* 2013, **84,** 330.
54. J. F. Kukowska-Latallo, E. Raczka, A. Quintana, C. Chen, M. Rymaszewski, and J. R. Baker, Jr., *Human gene therapy.* 2000, **11,** 1385.
55. C. S. O. Paulo, R. P. das Neves, and L. S. Ferreira, *Nanotechnology.* 2011, **22**.
56. Z. Amoozgar, and Y. Yeo, *Wiley interdisciplinary reviews. Nanomedicine and nanobiotechnology.* 2012, **4,** 219.
57. H. Hatakeyama, H. Akita, and H. Harashima, *Advanced drug delivery reviews.* 2011, **63,** 152.
58. S. Pamujula, S. Hazari, G. Bolden, R. A. Graves, D. D. Chinta, S. Dash, V. Kishore, and T. K. Mandal, *The Journal of pharmacy and pharmacology.* 2012, **64,** 61.
59. Y. Hu, J. Xie, Y. W. Tong, and C. H. Wang, *Journal of controlled release : official journal of the Controlled Release Society.* 2007, **118,** 7.
60. N. D. Sonawane, F. C. Szoka, Jr., and A. S. Verkman, *The Journal of biological chemistry.* 2003, **278,** 44826.

Figures:

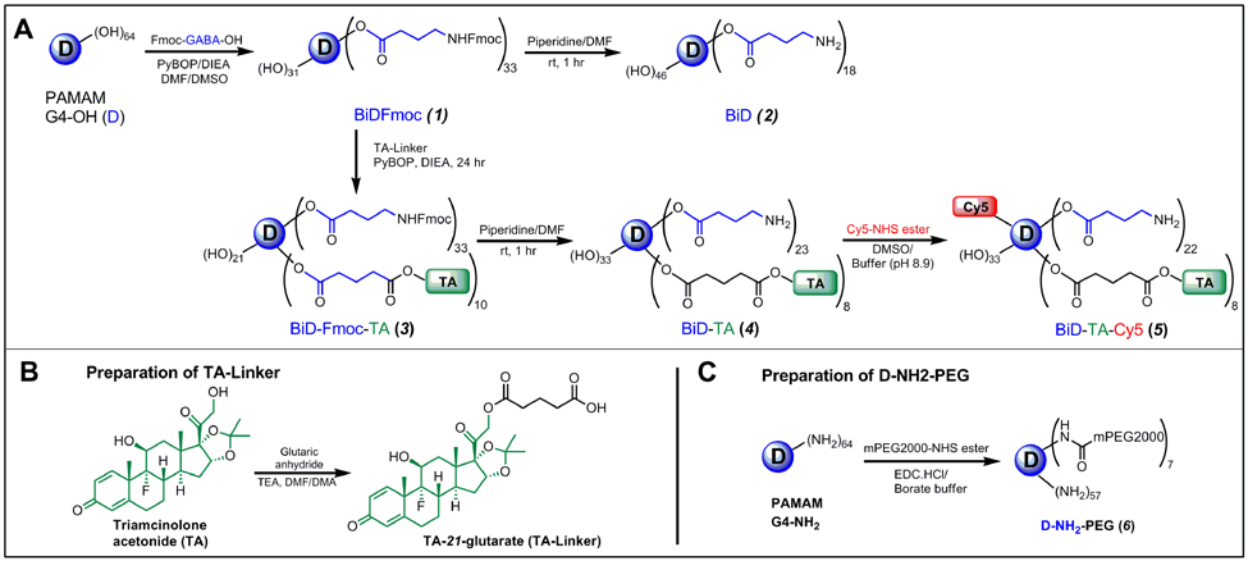

Figure 1: Preparation of the dendrimer conjugates. **(A)** Preparation of the amine functionalized bifunctional dendrimer (**BiD, *2***); Bifunctional triamcinolone acetonide (**BiD-TA, *4***); and Cy5-labeled bifunctional triamcinolone acetonide (**BiD-TA-Cy5, *5***). **(B)** Preparation of triamcinolone acetonide-21-glutarate (**TA-Linker**). **(C)** Preparation of PEGylated amine functionalized PAMAM dendrimer (**D-NH_2-PEG, *6***).

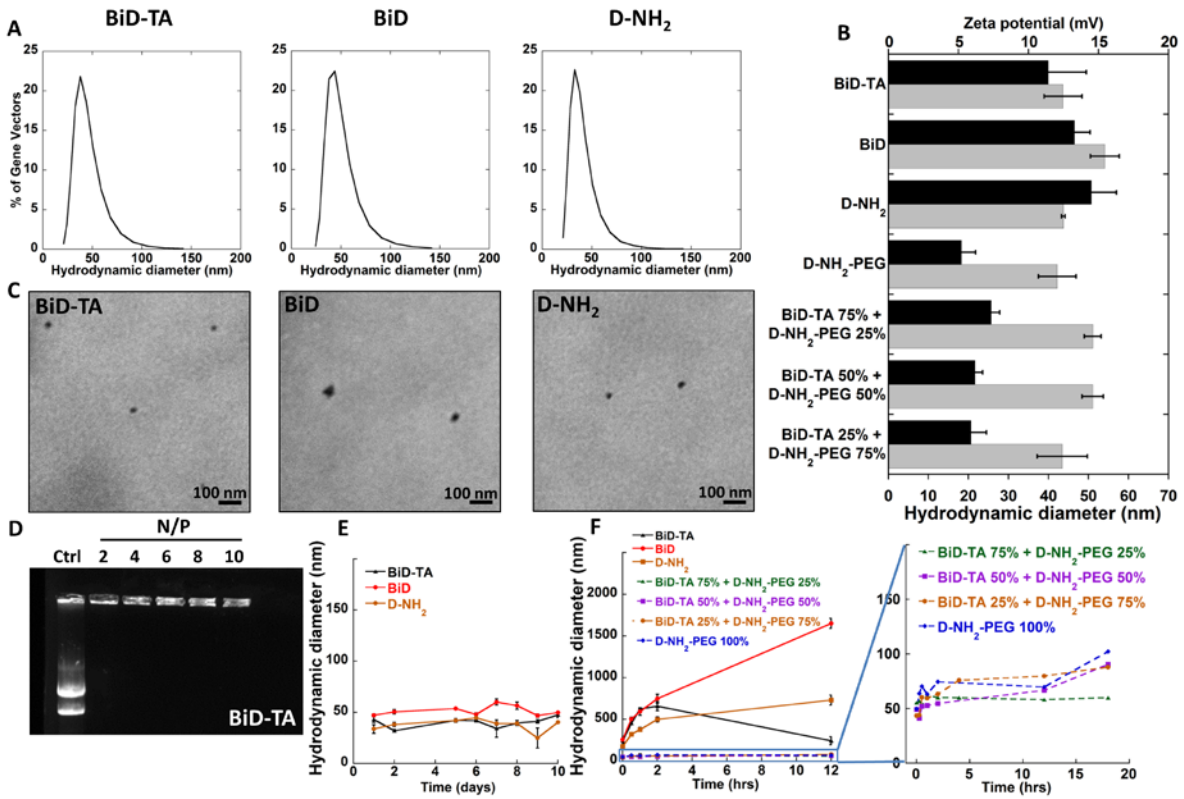

Figure 2: Gene vector characterization. (A) Hydrodynamic diameter distribution of respective gene vectors **(B)** Size and ζ-potential of respective gene vectors measured by dynamic light scattering (DLS) in 10mM NaCl at pH 7.0. Data are presented as average of at least 3 measurements ± standard error (SEM). **(C)** Transmission electron microscopy images of respective gene vectors in ultrapure water. **(D)** Gel retardation assay of BiD-TA gene vectors formulated at different N/P ratios. **(E,F)** Gene vector stability in ultrapure water **(E)** ad high ionic strength solution **(F)** using DLS to measure hydrodynamic diameter. Data are presented as average of at least 3 measurements ± (SEM).

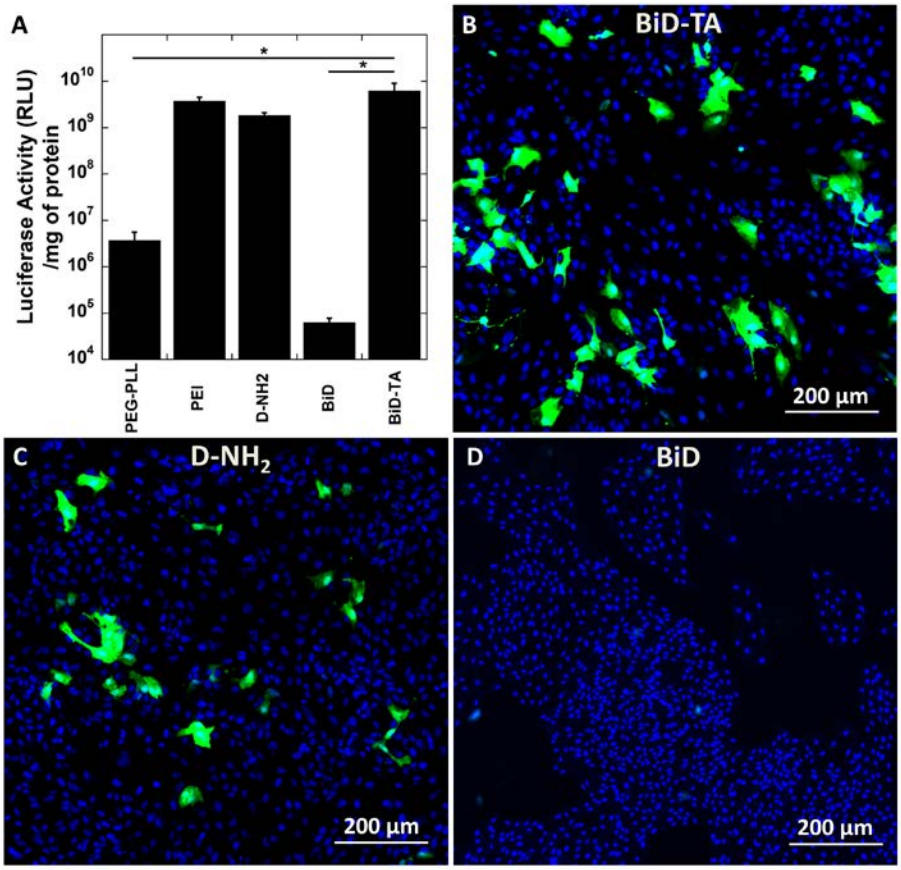

Figure 3: Transfection of human ARPE-19 cells by cationic polymer based gene vectors. (A) Luciferase activity following *in vitro* delivery of the luciferase gene to human ARPE 19 cells with respective gene vectors. Data represents mean ± SEM. * denotes statistical significance; $p<0.05$ **(B-D)** *In vitro* eGFP expression by ARPE cells following eGFP plasmid delivery using respective gene vectors.

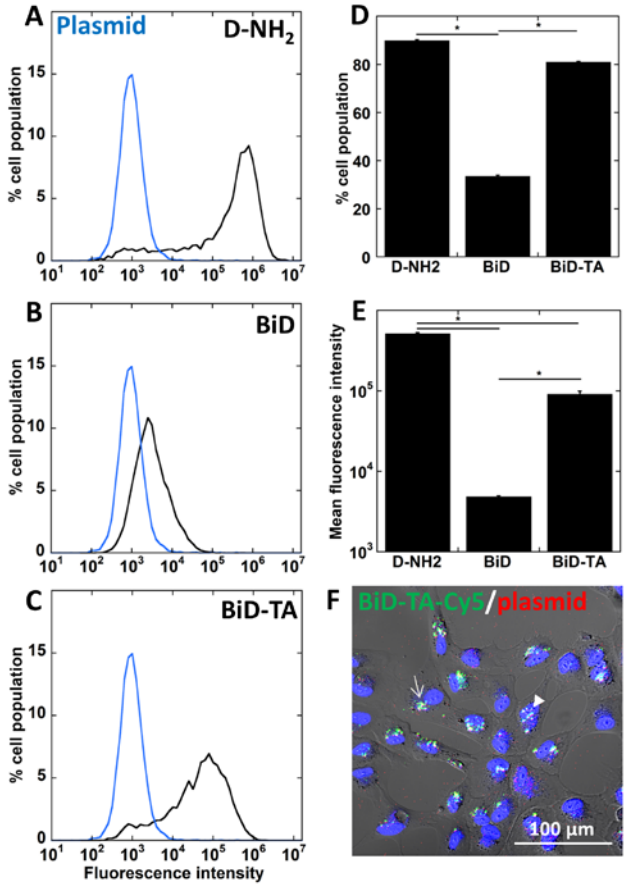

Figure 4: Gene vector uptake by human ARPE cells. (A-E) Flow cytometric analysis of fluorescently labeled gene vector cell uptake after 4 h of incubation with respective gene vectors. Data represents mean ± SEM. * denotes statistical significance; $p<0.05$ **(F)** Confocal imaging of BiD-TA gene vector cell uptake using dual fluorescent labeling. Dendrimer (Green), Plasmid (Red), Co-localization (Yellow). White arrow indicates gene vectors in the cytoplasm; white arrow head indicates gene vectors in the nucleus.

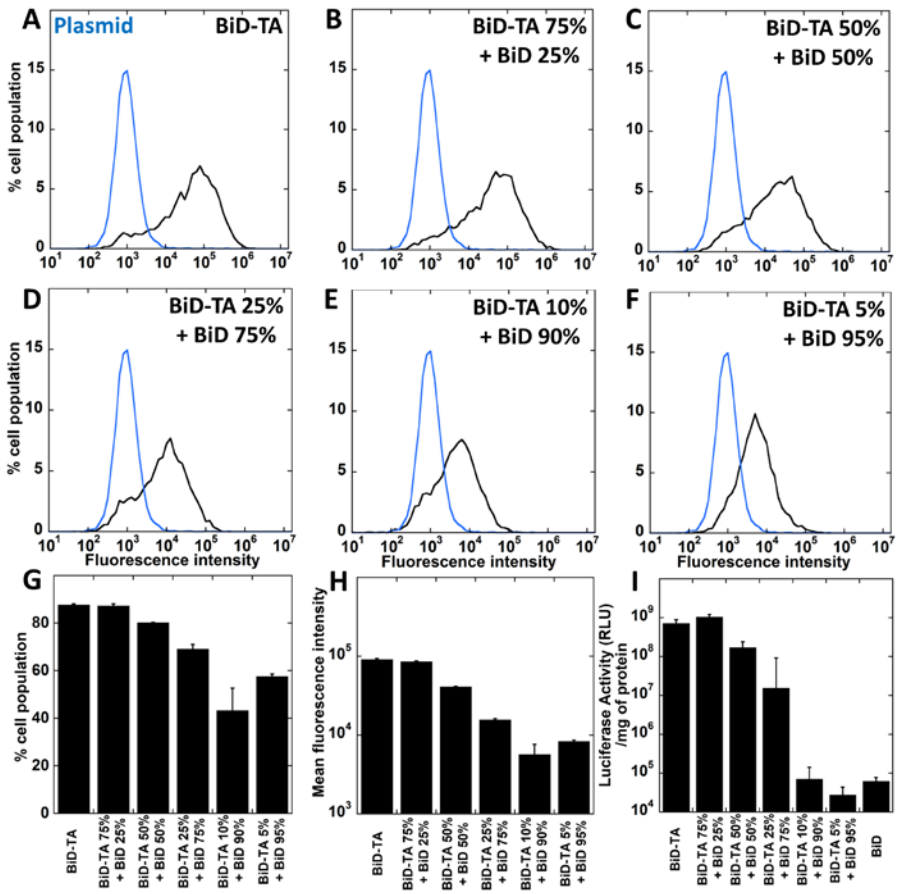

Figure 5: Effect of conjugated TA on gene vector cell uptake and transgene expression. (A-H) Flow cytometric analysis of cell uptake of fluorescently labeled gene vectors with varying ratios of BiD-TA/BiD. **(I)** Luciferase activity following *in vitro* delivery of luciferase gene to human ARPE 19 cells with respective gene vectors of varying BiD-TA/BiD ratios. Data represents mean ± SEM.

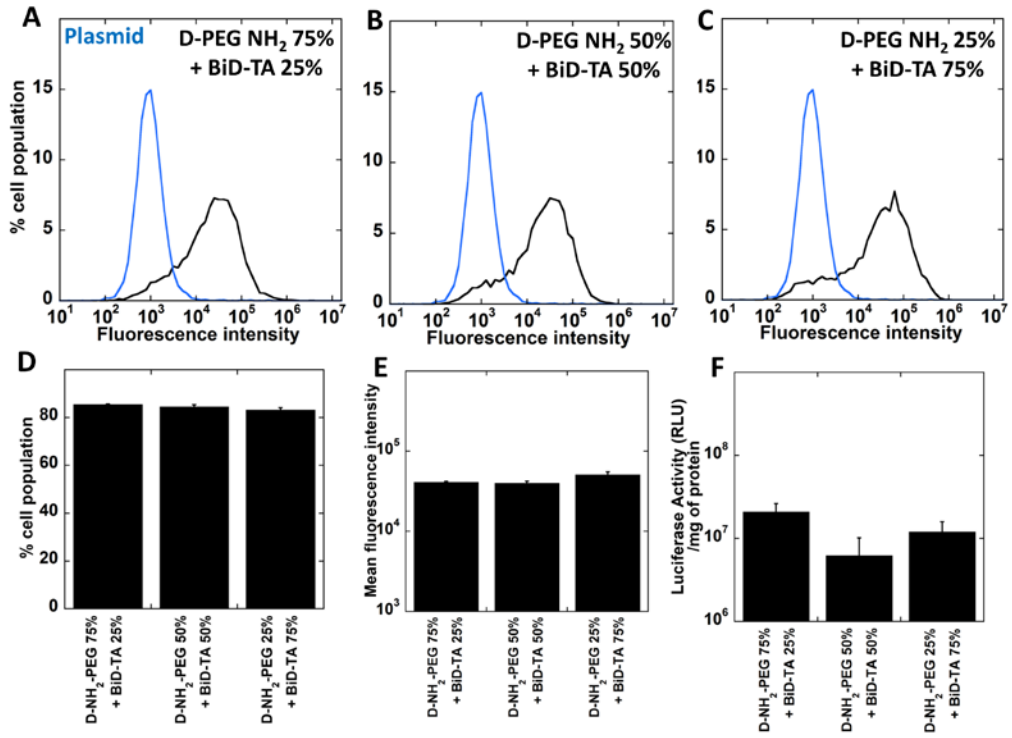

Figure 6: Effect of BiD-TA gene vector PEG coating on uptake and transgene expression. (A-H) Flow cytometry analysis of cell uptake of fluorescently labeled gene vectors with varying D-NH_2-PEG/BiD-TA ratio. **(I)** Luciferase activity following *in vitro* delivery of luciferase gene to human ARPE 19 cells with respective gene vectors of varying D-NH_2-PEG/BiD-TA ratio. Data represents mean ± SEM.

Gene vectors	Hydrodynamic diameter (nm) ± SEM	PDI	Zeta Potential (mV) ± SEM
BiD-TA	43.6 ± 4.7	0.20	11.4 ± 2.7
BiD	54.1 ± 3.6	0.16	13.3 ± 1.1
D-NH_2	43.7 ± 0.5	0.29	14.5 ± 1.8
D-NH_2-PEG	42.1 ± 4.7	0.24	5.2 ± 1.0
BiD-TA 75% + D-NH_2-PEG 25%	51.1 ± 2.1	0.26	7.3 ± 0.6
BiD-TA 50% + D-NH_2-PEG 50%	51.1 ± 2.7	0.24	6.1 ± 0.5
BiD-TA 25% + D-NH_2-PEG 75%	43.5 ± 6.3	0.25	5.9 ± 1.1

Table 1: Physicochemical characteristics of respective dendrimer-based gene vectors Size and polydispersity (PDI) were measured by dynamic light scattering (DLS). ζ-potential was measured by Laser Doppler anemometry. Measurements were performed in 10mM NaCl at pH 7.0 and are presented as average of at least 3 measurements ± standard error (SEM).